

Vortex pinning by compound defects in $\text{YBa}_2\text{Cu}_3\text{O}_{7-\delta}$

J. Hua,^{1,2} U. Welp,¹ J. Schlueter,¹ A. Kayani,³ Z. L. Xiao,^{1,2} G. W. Crabtree,¹ and W. K. Kwok¹

¹Materials Science Division, Argonne National Laboratory, Argonne, Illinois 60439, USA

²Department of Physics, Northern Illinois University, DeKalb, Illinois 60115, USA

³Department of Physics, Western Michigan University, Kalamazoo, Michigan 49008, USA

(Received 18 February 2010; revised manuscript received 30 May 2010; published 9 July 2010)

We investigate the enhancement of vortex pinning by compound defects that are composed of correlated and point defects in a pristine untwinned $\text{YBa}_2\text{Cu}_3\text{O}_{7-\delta}$ single crystal. Initial irradiation by high-energy heavy ions to a dose matching field of $B_\Phi=2.0$ T increases vortex pinning via columnar defects. Subsequent proton irradiation further enhances the critical current $J_c(H)$ by localizing the vortices near the columnar defects. Measurements of the shift of the irreversibility line for $H\parallel ab$ plane demonstrate that compound defects consisting of correlated and point disorder may reduce the pinning anisotropy and increase the overall critical current.

DOI: [10.1103/PhysRevB.82.024505](https://doi.org/10.1103/PhysRevB.82.024505)

PACS number(s): 74.25.Wx, 74.25.Uv, 74.25.Dw

The technology of high-temperature superconductors has greatly matured with the advent of second generation YBCO-coated conductors based on RaBiTs and IBA substrates.¹⁻⁴ These conductors are penetrating the commercial power industry with demonstrations of underground cables operating in urban grid systems. A limiting feature, particularly in high-field applications, is the anisotropy of the critical current and of the irreversibility line. This characteristic prompted the recent DOE-BES report on the basic research needs for superconductivity to identify the search for a high- T_c isotropic superconductor as one of the grand challenges of the field.⁵ One solution to this grand challenge is the search for new classes of superconductors with lower intrinsic superconducting anisotropy,⁶ such as the recently discovered superconducting iron pnictides.⁷⁻⁹ Another promising approach, which we elaborate here, is the modification of defect structures in the known cuprate superconductors to reduce their vortex pinning anisotropy by innovative pinning strategies. Correlated disorder such as naturally occurring twin boundaries, high-energy heavy-ion-induced columnar defects, and self-assembled nanodots to form nanorods are known to produce enhanced in-field vortex pinning along their long axis.¹⁰⁻¹² Although these studies are encouraging, their precise interpretation at the defect level is difficult because films and coated conductors already contain numerous defects such as microtwin boundaries, growth steps, textures, and substrate pinning among others, which confound the separation of the effective role of each specific defect.^{13,14}

Here we study the competition of vortex pinning effects due to compound disorder consisting of correlated defects introduced by heavy-ion irradiation and uncorrelated defects composed of point defects and their clusters created by proton irradiation. Unlike studies on thin films and coated conductors, we start from the “clean” limit using optimal-doped untwinned $\text{YBa}_2\text{Cu}_3\text{O}_{7-\delta}$ (YBCO) single crystals which display a clear first-order vortex melting transition, and sequentially introduce defects via particle irradiation. It is well known that columnar defects are one of the most efficient pinning centers because of their geometric match to the three-dimensional vortices in YBCO. They can significantly enhance the in-field critical current density and raise the irreversibility line.¹⁵ However, because of their correlated na-

ture, the pinning is highly anisotropic, as demonstrated by a sharp angular peak in J_c when the applied magnetic field is parallel to the direction of the correlated defects.¹⁰⁻¹² On the other hand, random point defects or their clusters such as those induced by chemical substitution or light particle irradiation can contribute to enhanced isotropic pinning behavior that does not generally induce additional anisotropy but may lower the irreversibility line.^{16,17} Although vortex pinning may not be additive, a combination of these two types of defects might be an effective method to tune the pinning anisotropy while increasing the overall pinning effect.^{12,18} Recent investigations on combining the effect of columnar and uncorrelated defects have relied on heavily doped crystals or films which already contain high concentrations of defects such as microplanar twin boundaries^{12,14} and atomic-scale defects leading to the ambiguity and complexity in separating the pinning contribution of each defect type. The use of pristine untwinned single crystals as a reference platform provides a systematic way to elucidate the separate contributions and interaction effects of correlated and point defects on transforming the pinning anisotropy of high-temperature superconductors. We directly demonstrate that the combination of columnar and point defects can be used to tune the irreversibility lines for $H\parallel c$ and $H\parallel ab$ by bringing them closer to each other while increasing the overall pinning strength.

High-purity YBCO single crystals were prepared using the flux-growth method and were mechanically detwinned by applying uniaxial pressure.¹⁹ No twin boundaries were observed under a polarized light microscope upon detwinning. A single crystal was polished down to about $70\ \mu\text{m}$ thickness along the c axis and cleaved into an $820\times 640\ \mu\text{m}^2$ rectangular piece. The zero-field superconducting transition temperature T_{c0} of the pristine YBCO crystal is 92.75 K. The crystal was irradiated with 1.4 GeV $^{208}\text{Pb}^{56+}$ ions at Argonne’s ATLAS heavy ion irradiation facility to a dose matching field of $B_\Phi=2.0$ T ($\sim 320\ \text{\AA}$ defect spacing) to create columnar defects along the crystallographic c axis. SRIM calculations²⁰ show that 1.4 GeV Pb irradiation does not fully penetrate through the $70\text{-}\mu\text{m}$ -thick crystal, leading to some splay in the columnar defect direction as the ions

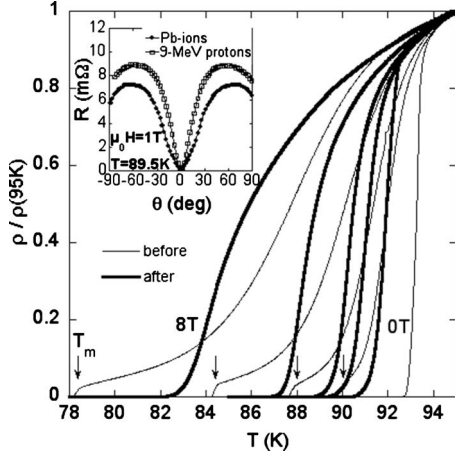


FIG. 1. Main panel: temperature dependence of the normalized resistivity $\rho(T)/\rho(95\text{ K})$ before (thin lines) and after (thick lines) heavy-ion irradiation in fields of 0, 1, 2, 4, and 8 $T \parallel c$. The arrows indicate the first-order vortex lattice melting transition of the pristine sample. Inset: angular dependence of the resistance of the crystal after heavy-ion irradiation (filled diamonds) and 9 MeV protons (open squares). Angles are measured with respect to the c axis.

come to a stop within the bulk of the crystal. Subsequently, the same crystal was irradiated at the tandem accelerator at Western Michigan University with (i) 9 MeV protons to a dose of $2 \times 10^{16} p/\text{cm}^2$ and with (ii) 6 MeV protons to a dose of $8 \times 10^{15} p/\text{cm}^2$. This series of proton irradiations produces point defects ($\sim 70\%$) and small clusters ($\sim 30\%$) with the size of $\sim 30 \text{ \AA}$.^{16,17} Standard four-probe transport measurements and magnetization measurements were performed using a Quantum Design physical properties measurement system (PPMS) and magnetic properties measurement system (MPMS), respectively, before and after each irradiation. For the magnetotransport measurements, the measuring current was applied in the ab plane. Transport measurements as a function of magnetic field direction were conducted with the sample placed on a rotator stage with a rotation precision of 0.05° with the applied field oriented perpendicular to the current in the maximum Lorentz force configuration.

The temperature dependence of the normalized resistivity before and after Pb-ion irradiation is compared in Fig. 1. The applied magnetic field ($0 \leq \mu_0 H \leq 8 \text{ T}$) is parallel to the crystallographic c axis. The sharp kinks in the resistance curves, indicated by the arrows, are associated with the first-order vortex freezing transition, which demonstrates the nearly defect-free nature of the untwined YBCO crystal before irradiation. This transition is completely suppressed and is replaced by a continuous transition which reaches zero resistivity at a much higher temperature after Pb ion irradiation to a dose matching field of $B_\Phi = 2.0 \text{ T}$. This behavior is consistent with the conclusion that the first-order transition disappears when $B_\Phi \geq 1.0 \text{ T}$ in optimal doped YBCO crystals.^{21,22} After subsequent irradiation with 9 MeV and 6 MeV protons the superconducting transition is lowered by $\sim 0.33 \text{ K}$ and $\sim 0.74 \text{ K}$, respectively, and the normal-state resistivity is increased by approximately 8% and 12%. These changes are associated with the increase in point-defect density.

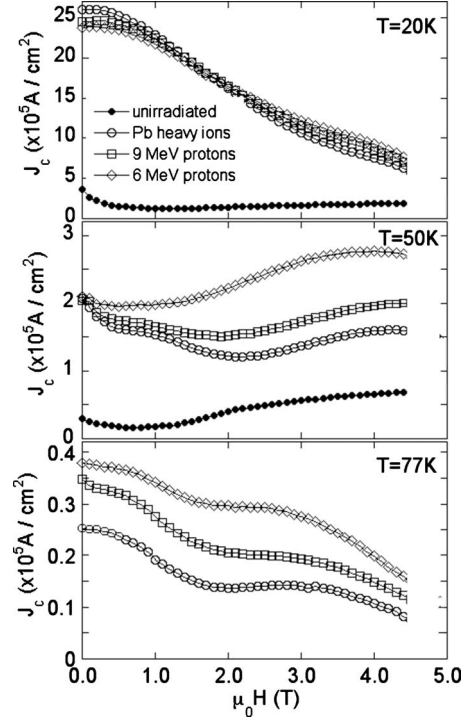


FIG. 2. Magnetic field dependence of the critical current density before and after irradiations for $T=20, 50,$ and 77 K for fields applied along the c axis. J_c of the pristine crystal at 77 K is essentially zero and is therefore not shown.

Figure 2 shows $J_c(H)$ for the unirradiated crystal and after each irradiation at various temperatures with the applied magnetic field along c axis. The critical current J_c (in units of A/cm^2) is determined using the Bean model,²³ for a rectangular-shaped sample, $J_c = 20\Delta M/w(1-w/3l)$, where ΔM is the magnetization hysteresis (in units of emu/cm^3), and w and l are the width and length of the sample, respectively, (in units of cm). In general, each successive irradiation significantly increases J_c over the entire temperature range from 20 to 87 K. At low temperatures near $T=20 \text{ K}$ and in fields below the dose matching field $B_\Phi = 2.0 \text{ T}$, the columnar defects induced by heavy-ion irradiation results in the highest J_c . There is a crossover behavior near $B > B_\Phi$ where proton irradiation results in a higher J_c . This behavior can be explained by the reduction in the effectiveness of columnar-defect pinning when vortices outnumber the defects at low temperatures when vortex creep is small. At 30 K this crossover occurs near 1.4 T and at higher temperatures where vortex creep is significant, the proton irradiation J_c curves lie above that of the heavy-ion irradiation curve at all fields. One remarkable observation is that when coexisting with columnar defects the point defects created by proton irradiation produce almost a doubling of J_c at higher temperatures. We note though that the absolute values of the 77 K- J_c shown in Fig. 2 are significantly smaller than those reported for state-of-the-art YBCO thin films and coated conductors.²⁴ This difference may arise from differences in defect concentration and topology and from contributions to the pinning force from interfacial and surface effects. Further studies are required to clarify this situation. Furthermore, a

strong second magnetization peak or “fishtail” effect is observed after Pb-ion irradiation that does not disappear after subsequent proton irradiation. In contrast, for pristine YBCO single crystals, the second magnetization peak is usually suppressed after successive proton irradiation.²⁵ The retention of the fishtail in our case suggests that the enhanced critical current following proton irradiation should not be understood as a simple addition of more pinning centers. The critical state of the vortex system in the presence of aligned columnar defects is prone to a fast decay due to the thermal excitation of vortex kinks and the easy motion of these kinks along the columnar defects.²⁶ Uncorrelated nanoparticle precipitates residing between self-assembled columnar defects have been shown to efficiently suppress the motion of the kinks and thereby increase the overall critical current and reduce the flux creep rate in BaZrO₃-doped YBCO thin films.¹² In our samples the pinning landscape consists of uncorrelated point defects and their clusters created by *p* irradiation and correlated columnar defects. This scenario of suppressed kink motion is consistent with the observation of the enhancement of the critical current at temperatures above 20 K, where vortex creep abounds and where compound defects, in particular, the point defects and their clusters induced by proton irradiation assist to reduce or suppress vortex creep, thereby increasing the critical current. However, at present, we cannot separate the pinning contributions arising from point defects and from clusters separately. Further studies using irradiation with electrons or neutrons which induce different defect distributions will clarify this question.

Shown in the inset of Fig. 1 is the angular dependence of the magnetoresistance for the crystal following high-energy Pb-ion irradiation and subsequent 9 MeV proton irradiation. A sharp resistivity minimum appears at *H*||*c* axis after Pb irradiation. Following the 9 MeV proton irradiation, the resistive minimum is—apart from the overall increase in the resistance—only slightly changed. The pronounced minimum in the magnetoresistance after 9 MeV proton irradiation demonstrates that the columnar defect pinning character of the crystal is retained, even though the critical current due to proton irradiation more than doubles.

The irreversibility line is an important characteristic boundary in the field-temperature phase diagram of high-temperature superconductors, which separates the mixed state into a magnetically irreversible vortex solid and a magnetically reversible vortex liquid region. Figure 3 shows the effect of the various defects on the irreversibility line defined by a resistivity criterion of $\rho=0.01 \mu\Omega \text{ cm}$. After Pb-ion irradiation, the irreversibility line is significantly shifted to higher temperatures compared to the first-order melting line before irradiation, even though the zero-field T_c has been reduced by 2.2 K. A kink feature on the irreversibility line separates a linear temperature dependence of $\mu_0 H_{irr}$ from a nonlinear region at about 2.0 T, which is very close to the dose-matching field B_Φ . A similar result has been reported for untwined YBCO crystals irradiated with 1.4 GeV U ions to dose matching fields of $B_\Phi=1, 2, \text{ and } 4 \text{ T}$.²⁷ The lower slope of the irreversibility line above $\mu_0 H=B_\Phi$ is caused by the reduction in the pinning efficiency of columnar defects when vortices outnumber the columnar defects.²⁸ The irreversibility lines as function of normalized temperature after

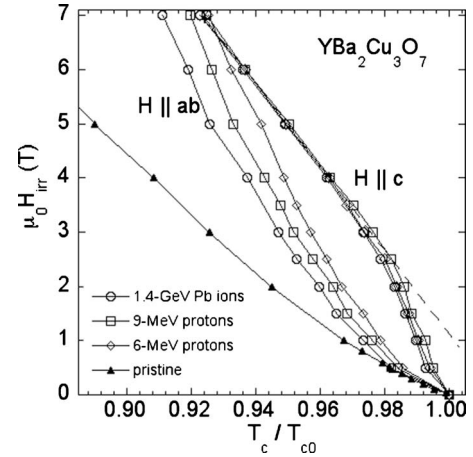


FIG. 3. Irreversibility lines after successive irradiation with heavy ions (circles), 9 MeV protons (squares), and 6 MeV protons (diamonds). The solid triangles indicate the vortex lattice melting line of the pristine sample. The dashed line represents an extrapolation of the linear T dependence of the c axis $H_{irr}(T)$ in fields larger than the dose matching field.

each successive irradiation are shown in Fig. 3. Note that following Pb-ion irradiation, the c -axis irreversibility line is shifted above the ab -plane irreversibility line, a consequence of the anisotropic pinning feature of the columnar defects. A similar result has been reported in the angular dependence of J_c for YBCO films containing self-assembled columnar defects.¹¹ Remarkably, subsequent proton irradiations do not change the c -axis irreversibility line (in reduced temperature), but instead, shift the ab -plane irreversibility line upwards. Our findings suggest that point defects may play a dual role when coexisting with columnar defects. For magnetic fields along the c axis, the point defects improve the high-field pinning of columnar defects below the irreversibility line by preventing vortex creep between the columnar defects resulting in an enhanced critical current. However, they do not increase the onset of pinning at the irreversibility line any further than established by the columnar defects. In contrast, for magnetic fields in the ab plane, the pinning strength of the columnar defects is greatly reduced due to unfavorable geometry (i.e., columnar defects perpendicular to vortices). Here, the random point defects provide the larger pinning strength, shifting the irreversibility line to higher temperatures and fields. As indicated by the shift of the ab -plane irreversibility line in Fig. 3 after each proton irradiation, our results show that a nearly isotropic pinning behavior (i.e., $H_{irr,||ab} \sim H_{irr,||c}$) may be achieved at $T=0.925T_{c0}$ and $\mu_0 H=7.0 \text{ T}$.

In conclusion, we have shown that a combination of correlated and point defects and clusters in the high-temperature superconductor YBCO can mitigate the anisotropy induced by high-pinning correlated disorder and yet further increase the overall critical current J_c . The retention of the fishtail in $J_c(H)$ indicates this combination is not simply an addition of pinning centers. Instead, point defects interact with correlated disorder to suppress the vortex creep between neighboring columnar defects. Point defects coexisting with columnar

defects may play a dual role by shifting the irreversibility line upward for $H\parallel ab$ and reducing vortex creep for $H\parallel c$ in our YBCO sample. Our study directly demonstrates an effective pathway to tune the anisotropic pinning while increasing the overall critical current in an inherently anisotropic high-temperature superconductor.

This work was supported by the Department of Energy,

Office of Basic Energy Sciences, under Contract No. DE-AC02-06CH11357 (U.W., J.S., and Z.L.X.), and by the Center for Emergent Superconductivity, an Energy Frontier Research Center funded by the U.S. Department of Energy, Office of Science, Office of Basic Energy Sciences under Award No. DE-AC02-98CH1088 (J.H., G.W.C., and W.K.K.).

- ¹A. Goyal, D. P. Norton, J. D. Budai, M. Paranthaman, E. D. Specht, D. M. Kroeger, D. K. Christen, Q. He, B. Saffian, F. A. List, D. F. Lee, P. M. Martin, C. E. Klabunde, E. Hartfield, and V. K. Sikka, *Appl. Phys. Lett.* **69**, 1795 (1996).
- ²C. P. Wang, K. B. Do, M. R. Beasley, T. H. Geballe, and R. H. Hammond, *Appl. Phys. Lett.* **71**, 2955 (1997).
- ³S. R. Foltyn, P. N. Arendt, Q. X. Jia, H. Wang, J. L. MacManus-Driscoll, S. Kreiskott, R. F. DePaula, L. Stan, J. R. Groves, and P. C. Dowden, *Appl. Phys. Lett.* **82**, 4519 (2003).
- ⁴R. A. Hawsey and D. K. Christen, *Physica C* **445-448**, 488 (2006).
- ⁵http://www.sc.doe.gov/bes/reports/files/SC_rpt.pdf
- ⁶A. Gurevich, Proceedings of M2S, Tokyo Japan, September 7–12, 2009 (unpublished).
- ⁷H. Takahashi, K. Igawa, K. Arii, Y. Kamihara, M. Hirano, and H. Hosono, *Nature (London)* **453**, 376 (2008).
- ⁸P. M. Grant, *Nature (London)* **453**, 1000 (2008).
- ⁹P. C. W. Chu, A. Koshchev, W. Kwok, I. Mazin, U. Welp, and H.-H. Wen, *Physica C* **469**, 313 (2009).
- ¹⁰J. L. MacManus-Driscoll, S. R. Foltyn, Q. X. Jia, H. Wang, A. Serquis, L. Civale, B. Maiorov, M. E. Hawley, M. P. Maley, and D. E. Peterson, *Nature Mater.* **3**, 439 (2004).
- ¹¹A. Goyal, S. Kang, K. J. Leonard, P. M. Martin, A. A. Gapud, M. Varela, M. Paranthaman, A. O. Ijaduola, E. D. Specht, J. R. Thompson, D. K. Christen, S. J. Pennycook, and F. A. List, *Supercond. Sci. Technol.* **18**, 1533 (2005).
- ¹²B. Maiorov, S. A. Baily, H. Zhou, O. Ugurlu, J. A. Kennison, P. C. Dowden, T. G. Holesinger, S. R. Foltyn, and L. Civale, *Nature Mater.* **8**, 398 (2009).
- ¹³L. Civale, B. Maiorov, A. Serquis, J. O. Willis, J. Y. Coulter, H. Wang, Q. X. Jia, P. N. Arendt, J. L. MacManus-Driscoll, M. P. Maley, and S. R. Foltyn, *Appl. Phys. Lett.* **84**, 2121 (2004).
- ¹⁴S. Awaji, M. Namba, K. Watanabe, T. Nojima, S. Okayasu, T. Horide, P. Mele, K. Matsumoto, M. Miura, Y. Ichino, Y. Yoshida, Y. Takai, E. Kampert, U. Zeitler, and J. Perenboom, *J. Phys.: Conf. Ser.* **97**, 012328 (2008).
- ¹⁵L. Civale, A. D. Marwick, T. K. Worthington, M. A. Kirk, J. R. Thompson, L. Krusin-Elbaum, Y. Sun, J. R. Clem, and F. Holtzberg, *Phys. Rev. Lett.* **67**, 648 (1991).
- ¹⁶L. M. Paulius, W.-K. Kwok, R. J. Olsson, A. M. Petrean, V. Tobos, J. A. Fendrich, G. W. Crabtree, C. A. Burns, and S. Ferguson, *Phys. Rev. B* **61**, R11910 (2000); A. M. Petrean, L. M. Paulius, W.-K. Kwok, J. A. Fendrich, and G. W. Crabtree, *Phys. Rev. Lett.* **84**, 5852 (2000).
- ¹⁷L. Civale, A. D. Marwick, M. W. McElfresh, T. K. Worthington, A. P. Malozemoff, F. H. Holtzberg, J. R. Thompson, and M. A. Kirk, *Phys. Rev. Lett.* **65**, 1164 (1990).
- ¹⁸G. W. Crabtree, W. K. Kwok, L. M. Paulius, A. M. Petrean, R. J. Olsson, G. Karapetrov, V. Tobos, and W. G. Moulton, *Physica C* **332**, 71 (2000).
- ¹⁹U. Welp, M. Grimsditch, H. You, W. K. Kwok, M. M. Fang, G. W. Crabtree, and J. Z. Liu, *Physica C* **161**, 1 (1989).
- ²⁰J. F. Ziegler, the stopping and range of ions in matter (SRIM), <http://www.srim.org/>
- ²¹N. Kobayashi, T. Nishizaki, K. Kasuga, and S. Okayasu, *Physica C* **460-462**, 1204 (2007).
- ²²W. K. Kwok, R. J. Olsson, G. Karapetrov, L. M. Paulius, W. G. Moulton, D. J. Hofman, and G. W. Crabtree, *Phys. Rev. Lett.* **84**, 3706 (2000).
- ²³C. P. Bean, *Phys. Rev. Lett.* **8**, 250 (1962); A. M. Campbell and J. E. Evetts, *Adv. Phys.* **21**, 199 (1972).
- ²⁴S. R. Foltyn, L. Civale, J. L. MacManus-Driscoll, Q. X. Xia, B. Maiorov, H. Wang, and M. Maley, *Nature Mater.* **6**, 631 (2007).
- ²⁵V. Tobos, L. M. Paulius, A. M. Petrean, S. Ferguson, J. W. Snyder, R. J. Olsson, W. K. Kwok, and G. W. Crabtree, *Appl. Phys. Lett.* **78**, 3097 (2001).
- ²⁶L. Krusin-Elbaum, L. Civale, J. R. Thompson, and C. Feild, *Phys. Rev. B* **53**, 11744 (1996); J. R. Thompson, L. Krusin-Elbaum, L. Civale, G. Blatter, and C. Feild, *Phys. Rev. Lett.* **78**, 3181 (1997); M. Konczykowski, V. M. Vinokur, F. Rullier-Albenque, Y. Yeshurun, and F. Holtzberg, *Phys. Rev. B* **47**, 5531 (1993).
- ²⁷R. J. Olsson, W. K. Kwok, L. M. Paulius, A. M. Petrean, D. J. Hofman, and G. W. Crabtree, *Phys. Rev. B* **65**, 104520 (2002).
- ²⁸L. Radzihovsky, *Phys. Rev. Lett.* **74**, 4923 (1995).